Formation and Reactivity of Silicon Oxyhydrides in Nickel Hydrogenation Catalysts Supported on Silica

Bram T. Kappé[1], Robin Vogel[1], Jaap N. Louwen[1], Bettina Baumgartner[1,2], Bert M. Weckhuysen[1,*], Matteo Monai[1,*]

[1] Inorganic Chemistry and Catalysis group, Institute for Sustainable and Circular Chemistry, Department of Chemistry, Utrecht University, Universiteitsweg 99, 3584 CG Utrecht, Netherlands

[2] Homogeneous, Supramolecular and Bio-Inspired Catalysis group, Van 't Hoff Institute for Molecular Sciences, Faculty of Science, University of Amsterdam, Science Park 904, 1098 XH Amsterdam, The Netherlands

*Corresponding authors: Bert M. Weckhuysen: B.M.Weckhuysen@uu.nl; Matteo Monai: M.Monai@uu.nl

Abstract: Silica is generally regarded as an inert support in the field of heterogeneous catalysis, including hydrogenation-dehydrogenation catalysis, on which hydrogen spillover is debated. Since supported hydrogenation and dehydrogenation catalysts are generally activated in H_2 as reducing gas at medium-high temperatures (350–500 °C), we suspected that hydride formation could occur during such catalyst pretreatments. In this work, we investigated silicon oxyhydride (SiH_xO_y, SiH_x for brevity) formation during the reduction pretreatment of a set of Ni/SiO_2 catalyst materials using in situ diffuse reflectance infrared Fourier transform spectroscopy (DRIFTS). We observed two distinct vibrational bands located at ~ 2275 and ~ 2257 cm^{-1}, which we assigned to SiH and SiH_2 species, as supported by density functional theory (DFT) calculations. Since these vibrational bands are absent after hydrogenation of pure silica, we propose that the formation of hydrides was caused by hydrogen spillover from Ni metal nanoparticles supported on silica. The decrease in the band areas with rising temperature was used in a van t 'Hoff plot to yield enthalpy values of ~ 26 and ~ 42 kJ/mol for the apparent reaction of hydride species, suggesting an equilibrium with IR-inactive or very mobile species. The reactivity of the SiH_x species was also investigated, by dosing methanol, water and CO_2 as probe molecules on the pre-reduced Ni/SiO_2 catalysts. Methanol reacted the fastest with the hydride species, followed by water, while CO_2 did not show any interaction with the hydrides. We anticipate this work will contribute to changing the view of silica as an inert support material, and to the understanding of H spillover in more general.

Introduction

In heterogeneous catalysis, supports are used as physical carriers for the active phase thereby providing stability and isolation of active sites, as well as to tune the electronic and structural properties of active sites.[1] One of the most common catalytic supports is silica (SiO_2), which is generally regarded as a stable, non-reducible, and inert porous support in comparison to reducible supports, such as ceria, niobia, and titania, which have active sites known to cooperate during catalysis.[2] One example of cooperative catalysis is the adsorption of reactants at the metal/oxide interface: in CO_2 hydrogenation, CO_2 can adsorb on oxygen vacancies of ceria to form carbonate species, which can react further to methane in close proximity to the active phase.[3] In contrast, SiO_2 is mostly considered inert, with the catalytic CO_2 hydrogenation reaction believed to occur only on the Ni surface.[4]

A widespread example of chemical metal/support interaction is hydrogen spillover. Hydrogen spillover was first reported in 1964 for a Pt/WO_3 system and involves the migration of hydrogen activated on the active metal over the support.[5,6] Hydrogen spillover is well-accepted for reducible supports, such as CeO_2, TiO_2, WO_3, MoO_3 and nanostructured ZrO_2.[6,7] For non-reducible supports, such as SiO_2, MgO and Al_2O_3, however, hydrogen spillover is heavily debated.[6,8-11] Some studies claimed to observe hydrogen spillover on Al_2O_3 and SiO_2, for example by the exchange of -OH with -OD groups on Rh/Al_2O_3 upon D_2 activation on Rh.[8] Moreover, spillover of *H from Pt to FeO_x over Al_2O_3 was observed using X-ray absorption spectro-microscopy, albeit 10 orders of magnitude slower and over shorter distances than across TiO_2.[9] Additionally, *H spillover from Pt over SiO_2 was used to explain an increase in CO_2 hydrogenation rates on $Pt\text{-}Co/SiO_2$ catalysts compared to Co/SiO_2.[10] However, as discussed by Prins, H-D exchange alone is not sufficient proof of *H spillover, as H-D exchange can take place without net movement of H/D atoms.[6] Furthermore, *H spillover onto non-reducible supports was claimed to be unlikely since the interaction between *H and these supports was very weak, or even negative (repulsive) in the case of SiO_2.[11]

The nature of spilled-over and absorbed H is discussed in a few studies. There are three main types of adsorbed hydrogen proposed in literature: (i) *H with a negative charge, called hydride or said to have hydridic character; (ii) *H with a positive charge, i.e., a proton; and (iii) so-called "atomic" *H, claimed to be formed as a result of homolytic cleavage of H_2 over metal surfaces, yielding two M-H species. However, since hydrogen is more electronegative compared to many transition metals, it was shown that even following homolytic cleavage of H_2, *H does gain some electron density from the surface, making it partially negatively charged (hydridic). For example, in the 1960s and 1970s, magnetization studies of H_2 adsorption on Ni/SiO_2 reported 'appreciable density around the hydrogen nucleus' and the adsorbed *H acquiring some negative charge.[12–14] A density functional theory (DFT) study found a decrease in density of states (DOS) around the Fermi level upon adsorption of H_2 on Pd, which can be explained by transfer of electron density from Pd to H, leading to hydridic *H formation. Therefore, homolytic cleavage of H_2 on most transition metals yields two metal hydrides. For bulk oxides, *H can exist on the support in both the form of a proton (e.g., Ti-OH) or hydride (e.g., Ce-H or Al-H).[9,15,16] In supported metal catalysts, heterolytic cleavage of H_2 is also possible at a metal/support interface on frustrated-Lewis-pairs, yielding a hydride and a proton, often in the form of a hydroxyl group.[17,18]

All considered, this suggests that hydrides could be involved in *H spillover in silica-supported catalysts. Interestingly, this was not considered in the DFT study by Prins

et al.[11] Hydrides on silica were reported in literature under several names: silicoformic anhydride, silicon oxyhydrides, (hydro)silanes and surface silicon hydrides.[19,20] Silicon oxyhydrides (SiH_xO_y, referred to as SiH_x herein for brevity) were first synthesized by Buff and Wohler in 1857 by hydrolysis of trichlorosilane, although it was not clear what the exact structure of the resulting oxide was at the time.[19,21] Later on, the material was characterized as SiO_2 with a hydrophobic coating of silicon oxyhydride.[19,22] Silicon oxyhydrides prepared through hydrolysis of trichlorosilane were later used as catalysts for hydrosilylation of olefins.[23]

Hydrides on bulk oxides can be studied with infrared (IR) spectroscopy, nuclear magnetic resonance (NMR), X-ray photoelectron spectroscopy (XPS) and neutron scattering (NS).[20,24] Silicon oxyhydrides were first characterized using IR spectroscopy in 1968, with a band located at ~ 2300 cm^{-1}, being assigned to SiH_2 species.[25] The material was synthesized through pyrolysis of silica treated with methanol yielding a 'reactive silica' which was thought to contain strained Si-O-Si bonds and SiH_2 species.[25] Treatment of the 'reactive silica' with H_2 gave rise to another band at ~ 2227 cm^{-1}, which was assigned to a silicon oxyhydride species.[26] Silicon oxyhydrides resulting from dichlorosilane hydrolysis were also studied with IR spectroscopy, and showed bands between 2200 and 2300 cm^{-1}, which have been assigned to the Si-H stretching vibrations.[27] More controlled hydrolysis of dichlorosilane in dichloromethane yielded cyclic $[H_2SiO]_n$ oligomers, which were characterized by IR spectroscopy to have Si-H vibrations at 2200 or 1195 cm^{-1}, and Si-H bending vibrations between 1000 and 900 cm^{-1}.[28] Silicon oxyhydrides were first characterized by ^{29}Si solid-state NMR in 1981, showing a signal at -85.0 ppm.[29] They were also observed with IR spectroscopy and by NMR after decomposition of organometallic Zr, W, Ta and Zr complexes supported on SiO_2 under hydrogen.[30–34] Silicon oxyhydrides were also formed by heating silica gel in H_2 to 800 °C in the presence of metal impurities (e.g., Ta, Ni, Pt, and W) which the authors presumed to be through spillover.[35]

Summarizing, there is experimental evidence of hydrogen spillover on reducible supports playing a role in the field of heterogeneous catalysis. For the 'inert' support SiO_2 this is thought not to be the case, although there are several reports of hydrides existing on silica. Despite SiO_2 being one of the most commonly used support materials, it is unclear whether hydrides are formed during reduction, as there are no in situ spectroscopy studies focused on this phenomenon. If there are hydrides formed on silica, these could influence catalytic behavior. Furthermore, the reactivity of silicon oxyhydrides has not been studied in depth. In this work, we report on the formation of silicon oxyhydrides after reduction of $NiCO_3/SiO_2$ precatalysts to Ni/SiO_2, and we study the hydrides thermal behavior and reactivity towards water, methanol and CO_2 by in situ diffuse reflectance infrared Fourier transform spectroscopy (DRIFTS).

Results and Discussion

To explore the possible formation of silicon oxyhydrides on Ni-based hydrogenation catalysts, we have selected a set of Ni/SiO_2 catalysts having different loadings and nickel nanoparticle sizes, which were previously tested in CO_2 and ethylene hydrogenation.[36] According to temperature programmed reduction (TPR) results, and based on established activation methods for Ni/SiO_2 catalysts, we have reduced the $NiCO_3/SiO_2$ pre-catalyst materials to Ni/SiO_2 in 50 vol.% H_2/N_2 at 550 °C for 1 h. After reduction, the atmosphere was switched to pure N_2 and the catalyst materials were cooled to room temperature. Using the DRIFTS technique we observed Si–O vibrational overtones and combination bands for both Ni/SiO_2 catalysts and a SiO_2 reference (**Fig. 1A**, 'SiO_2' region).[37] On the Ni/SiO_2 catalysts, however, two bands at ~ 2275 and ~ 2257 cm^{-1} were observed (**Fig. 1B**, bands '**a**' and '**b**' respectively), which were not present after reduction of Ni-free SiO_2.

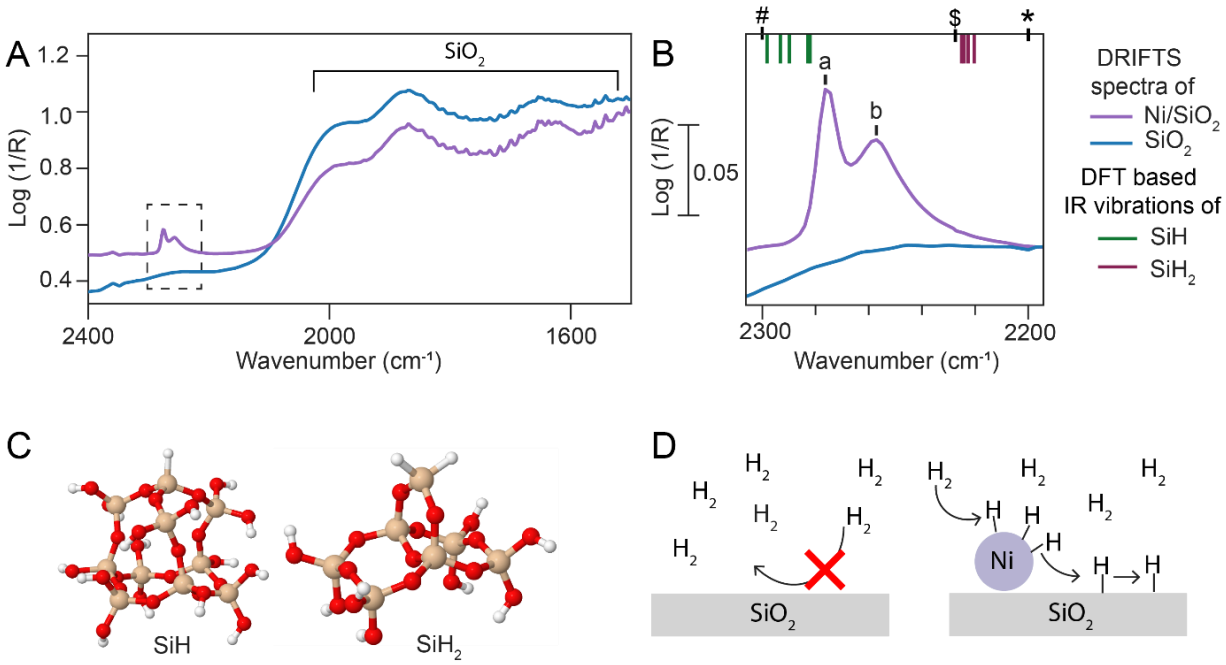

Figure 1. Silicon oxyhydride formation in Ni/SiO_2 catalyst materials upon reduction pretreatments. (**A**) Diffuse Reflectance Infrared Fourier Transform Spectroscopy (DRIFTS) results for Ni/SiO_2 (11.8 wt.% Ni/SiO_2, with a 2.1 ± 1.1 nm mean Ni nanoparticle (NP) size) and SiO_2 at 25 °C, after reduction in 50 vol.% H_2/N_2 at 550 °C for 1 h. For Ni/SiO_2, bands at ~ 2275 and ~ 2257 cm^{-1} are observed, which are assigned to SiH and SiH_2 vibrations, respectively. Bands in the 2000–1500 cm^{-1} region are assigned to overtones of SiO_2 framework vibrations. A zoom-in of the dashed box is reported in (**B**), showing the two observed infrared (IR) bands (a, b) together with the SiH and SiH_2 IR band positions, as calculated by Density Function Theory (DFT) and the reported positions of SiH_2 (**#**)[25] and SiH (**$**)[26], (*)[28] in literature. (**C**) Representative optimized DFT models of SiH and SiH_2 species. All models considered can be found in the Supporting Information (SI). (**D**) Scheme of the proposed formation of hydrides on silica via * H spillover from Ni.

The positions of the observed bands are consistent with the previously reported stretching vibrations of silicon oxyhydrides, as discussed in the introduction.[25,26,28] To corroborate our IR spectral interpretation, we used DFT to calculate the IR band positions of SiH and SiH_2 species on silica models, consisting of 6 to 10 Si atoms (**Fig. 1C**). All models considered can be found in the Supporting Information (SI), **Fig. S1**. For all calculations, we used the B3LYP density functional[38] and the 6-31+G** basis

set.[39] The calculated IR frequencies were scaled by scaling factors to match the observed and computed frequencies of SiH_4. More details on the computational procedure can be found in the SI, Section **S1**. Si-H stretching modes with frequencies in the spectral regions 2299–2283 and 2220–2225 cm^{-1} were found for the SiH and SiH_2 models, respectively. These values are relatively higher and lower than our experimentally observed values of ~ 2275 and ~ 2257 cm^{-1} (**Fig. 1B**), with a difference of ~ 15–30 cm^{-1}, which are usual errors in DFT calculated IR bands positions. Based on DFT and literature, we thus assign band '**a**' at 2275 cm^{-1} to SiH species and band **'b'** at 2257 cm^{-1} to SiH_2.

Since the SiH_x species require Ni to be formed, we hypothesize that H_2 dissociates to hydrides on Ni at high temperatures under H_2/N_2 atmosphere, after which the Ni hydrides spill-over to the silica support, as shown in **Fig. 1D**. Accordingly, we calculated a single adsorbed *H on Ni(100) to gain 0.27 electrons, thus forming a hydride as expected from differences in electronegativity between H and Ni. An alternative hypothesis involves heterolytic of cleavage of H_2 at a metal-support interface, which was proposed for Au/TiO_2 for example.[40,41] Heterolytic cleavage at a Ni/SiO_2 interface could cause a proton to react with a Si-OH group to form water, which could desorb and leave a vacancy for the hydride on Ni to spill over to, forming the silicon oxyhydride species. As discussed in the Introduction part, *H spillover onto silica is debated, as it was found unfavorable in theoretical calculations when modelling *H as a proton, forming OH groups.[10,11] We here instead observed *H residing on a silica surface in the form of a hydride, explaining the discrepancy between experiments and DFT calculations.

However, it remains unclear how these envisaged H* spillover phenomena exactly happen. We hypothesize that hydrides on Ni react with Si-OH to form Si-H and water according to Eq. (1):

$$2H^* + \text{Si-OH} \leftrightharpoons \text{Si-H} + H_2O \quad (1)$$

where Si-OH can be one of many types of hydroxyl groups present on silica, known to have a complex surface chemistry.[42] Another possible reaction pathway involves defects or strained Si-O-Si groups:[42,43]

$$2H^* + \text{Si-O-Si} \leftrightharpoons \text{Si-H} + \text{Si-OH} \quad (2)$$

Indeed, H_2 is known to react with defects in silica which have dangling bonds or "E' centers", to form SiH groups, which is an important effect in the manufacturing of Si/SiO_2 semiconductor devices.[44] Accordingly, **Fig. S3** shows the DRIFTS spectra of Ni/SiO_2 during and after reduction, in which a sharp band at ~ 3736 cm^{-1} is formed, which can be assigned to free Si-OH groups, and a broad band in the 3300–3700 cm^{-1} region, which is likely due to H-bonded (vicinal) Si-OH groups and adsorbed water.[42,43,45]

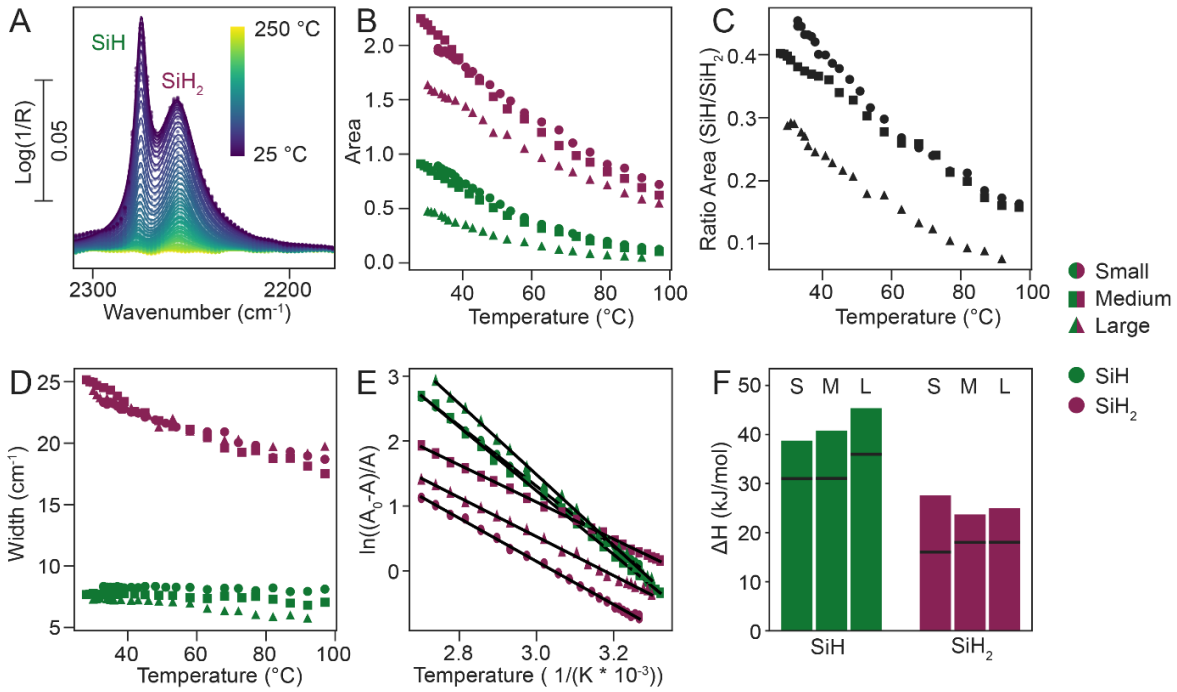

Figure 2. Thermal behavior of silicon oxyhydrides on Ni/SiO_2 catalysts. (**A**) Background-corrected infrared (IR) spectra of 11.8 wt.% Ni/SiO_2 with a Ni nanoparticle size of 2.1 nm (medium), as a function of temperature, showing the SiH_x bands region (shown as datapoints) together with fitting results using two Lorentzian functions (see section 2 of the Supporting Information (SI) for further details on the data analysis procedure used). (**B–D**) Fitting results for the two SiH_x bands versus temperature for three Ni/SiO_2 catalyst materials having different weight loading (i.e., 4.2, 11.8, and 19.5 wt.%) and Ni nanoparticle (NP) sizes (i.e., 1.2 ±0.5, 2.1 ±1.1, and 4.4 ±2.4 nm, small, medium and large, respectively): (B) band area, (C) ratio, and (D) width of SiH vs. SiH_2 band areas versus temperature. (**E**) van 't Hoff plot for the disappearance of the SiH_x bands (for details on A_0 definition, see SI). (**F**) Enthalpy values derived from van 't Hoff plot for the apparent reaction of SiH_x species, for optimal A_0 values (bars) and A_0 of 10x A at 25 °C (lines in bars).

Since many catalytic hydrogenation reactions are carried out at temperatures in the range of 50–400 °C, we studied the thermal stability of silicon oxyhydrides, by investigating the temperature-dependent behavior of the SiH_x bands. Notably, in all experiments, we switched the gas atmosphere after reduction from H_2/N_2 to pure N_2 at 550 °C before cooling down, which means that *H species must have formed at high temperature when H_2 was available. However, the SiH_x IR bands only became visible when cooling below ~150 °C (**Fig. 2A**). This behavior was reversible with temperature: when the temperature was raised again in N_2, the bands disappeared, and re-appeared again when the temperature was lowered.

The reason for the reversible decrease of the area of the SiH_x bands with rising temperature is not immediately clear and required further data analysis. The decrease of the area of the SiH_x bands with rising temperature was quantified with a spectral fitting procedure, to gain more insight in this behavior. We have fitted the SiH_x bands of three Ni/SiO_2 samples (average Ni particle size of 1.2, 2.1 and 4.4 nm, referred to as 'small', 'medium' and 'large') as two Lorentzian functions to a background-corrected spectrum. For details, please refer to the Section **S2** of the SI. The fitting results are presented in **Fig. 2B–D**, in terms of band area, relative area and width.

For all the Ni/SiO_2 catalyst materials studied in this work, the band areas of both the SiH and SiH_2 peaks dropped with increasing temperature (**Fig. 2B**), while the position of the IR bands did not change significantly (**Fig. S4**). The ratio of the two band areas (SiH band/SiH_2 band) decreased with temperature, because the area of the SiH band decreased faster compared to the area of the SiH_2 band (**Fig. 2C**). Overall, the different behavior of the two bands reinforces the assignment to two separate species.

In literature, the disappearance of SiH_x IR bands on silicon was ascribed to dephasing of the band by anharmonic coupling to the Si-H bending vibrations around 800 cm^{-1}.[46] However, in such case a concomitant IR band broadening was observed, while in our case a slight band narrowing occurred for the SiH_2 species from 25–100 °C (**Fig. 2C**). This suggests that dephasing is unlikely to be the case of SiH_x band intensity drop with temperature.

An alternative hypothesis for the decrease in band area is an increased mobility of *H with temperature. In the field of applied physics, hydrogen diffusion across silicon and silica surfaces was studied extensively.[47] For example, the photo-induced formation of a metastable, weakly bound silicon hydride, which can diffuse rapidly on the silicon surface, is believed to be the cause of the Staebler-Wronski effect, which influences silicon conductivity.[47–49] Interestingly, the effect is reversible when heating to 150 °C, the same temperature where we observed the SiH_x bands to completely disappear.[49,50] Hydrogen diffusion through a Si/SiO_2 interface was also observed, and it was noted that *H was diffusing through SiO_2 as well as trough Si, although at a much slower rate.[51]

It is, however, unclear how SiH_x would become mobile in our case, in the absence of photo-excitation. We thus hypothesized that a chemical equilibrium could be responsible for the disappearance of the SiH_x IR bands with temperature, where SiH_x species are either reversibly converted to a highly mobile species or to IR inactive species upon heating. To test our hypothesis, we used van ‘t Hoff plots to analyze the fitted data and gather insights on the thermodynamics of the system (**Fig. 2E**).

Assuming an equilibrium is established between an IR-active species A and an IR-inactive species B, we can write the equilibrium constant, K, as:

$$K = \frac{[B]}{[A]} \tag{3}$$

Based on the stoichiometry of the reaction, and assuming that no side reactions occur, K can be also written as:

$$K = \frac{[\mathrm{A}]_0 - [\mathrm{A}]}{[\mathrm{A}]} \tag{4}$$

where $[\mathrm{A}]_0$ is the concentration of A when the equilibrium is completely shifted to the left, and no B is formed. This value is in principle not known, but can be found iteratively (see Section **S3** of the SI for further details). Assuming that the enthalpy and enthalpy change of the reaction is not temperature dependent in the considered conditions, we can use the van ‘t Hoff relationship as written in Eq. 5.

$$ln\, K = \left(\frac{-\Delta H^\circ}{RT}\right) + \left(\frac{-\Delta S^\circ}{R}\right) \tag{5}$$

And therefore, by plugging Eq. 4 into Eq. 5:

$$ln\left(\frac{[\mathrm{A}]_0 - [\mathrm{A}]}{[\mathrm{A}]}\right) = \left(\frac{-\Delta H^\circ}{RT}\right) + \left(\frac{-\Delta S^\circ}{R}\right) \tag{6}$$

Assuming the validity of the Lambert-Beer law (or in other words, a proportionality between species concentration and their IR absorbance), the IR band area of the SiH_x

species A is proportional to [A]. By plotting ln((A$_0$-A)/A) versus 1/T, one can therefore derive the ΔH of the apparent equilibrium of A ⇋ B from the slope of a linear fit of the data. Normally one would be able to obtain the ΔS value from the intercept with the y axis. However, in our case the ΔS value cannot be obtained since we do not know the extinction coefficient of species A or B, so we do not know the absolute value of [A], only the change which is described in the slope.

The apparent enthalpy of reaction of the SiH and SiH$_2$ species, as shown in **Fig. 2F**, calculated based on the slope of the van 't Hoff plots, facilitates the interpretation of their behavior. The enthalpy values obtained are positive, as expected for an endothermic equilibrium, and between 39–45 kJ/mol for SiH, and between 24–28 kJ/mol for SiH$_2$. These values are an order of magnitude smaller compared to the energy of a covalent bond, but are comparable to weaker interactions, such as hydrogen bonding. In literature, values of 20–25 kJ/mol were calculated for interaction of H$_3$SiOH with water.[52] Therefore, a possible explanation for the endothermic process responsible for the decrease in band area is that hydrogen bonding of Si-OH groups or adsorbed water surrounding the SiH$_x$ species at low temperatures prevents the SiH$_x$ species to move freely. When the temperature is raised, such H-bonds are broken, and *H species can become mobile on the silica surface.

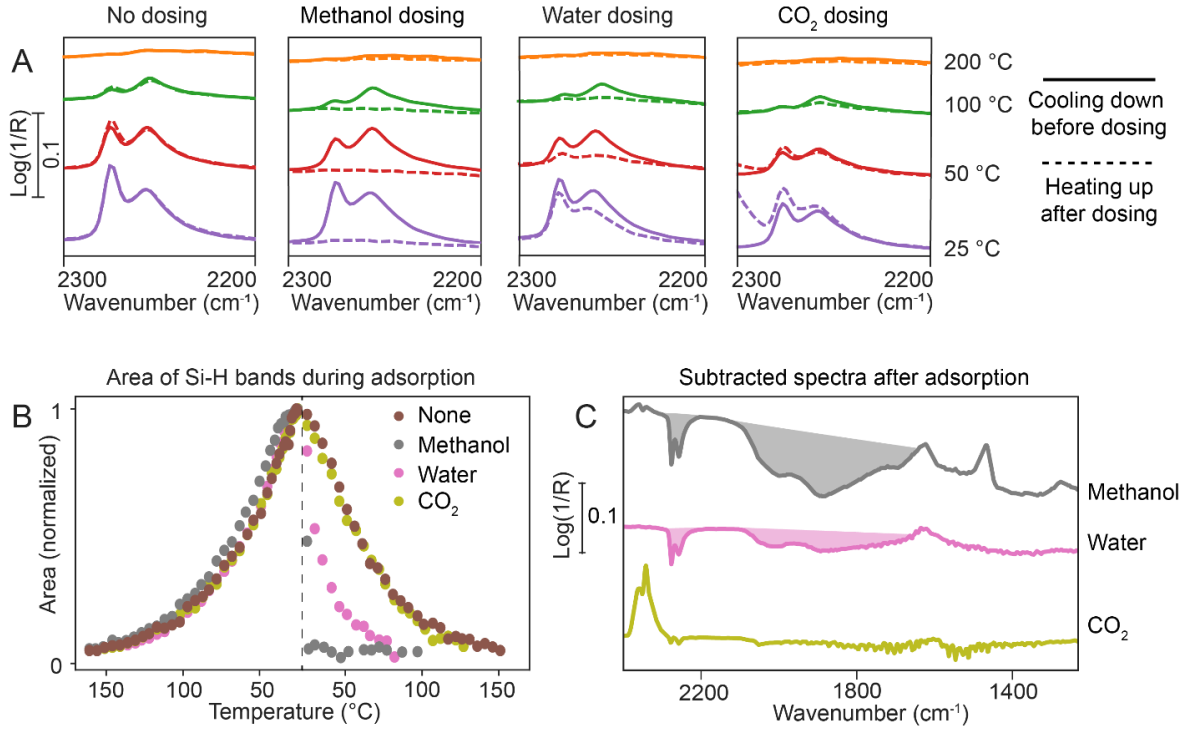

Figure 3. **Reactivity of silicon oxyhydrides on Ni/SiO$_2$ catalysts studied with various probe molecules.** (**A**) Diffuse reflectance infrared Fourier transform spectroscopy (DRIFTS) spectra of probe molecules adsorption experiments on a pre-reduced 11.8 wt.% Ni/SiO$_2$ catalyst. The catalysts were cooled down in N$_2$ after reduction (solid lines), exposed to the probe molecule at 25 °C, and then heated to 400 °C in N$_2$ (dashed lines). From left to right: reference experiment in N$_2$, and methanol, water or CO$_2$ as probes. (**B**) Normalized area of both SiH$_x$ bands over time during probe molecule experiments. The probe molecules were introduced at 25 °C (dashed line). (**C**) DRIFTS spectra after exposure to methanol, water or CO$_2$, and subsequently recorded at 40 °C and subtracted with a reference spectrum recorded at 40 °C after reduction during each experiment. The shaded areas indicate the negative bands observed after subtraction, due to removal of SiH$_x$ species and changes in the Si-O-Si vibrations.

The presence of hydrides on Ni/SiO_2 raises questions about their reactivity, and whether they potentially play an active role in heterogeneous catalysis. Not much is known yet about the reactivity of silicon oxyhydrides. SiH_4 and silicon hydrides on silicon nanocrystals were shown to react with CO_2 to form silica, and C or CO.[53,54] However, silicon oxyhydrides were not active for converting CO_2 into CO.[53] To gain more insight into the reactivity of silicon oxyhydrides, we exposed reduced Ni/SiO_2 catalyst materials to probe molecules, such as water, CO_2 and methanol, and observed the subsequent changes in the SiH_x band intensity as a function of reaction temperature and the type of probe molecule (**Fig. 3A,B**).

In a typical experiment, the catalyst was reduced at 550 °C for 1 h, after which the gas stream was switched to N_2 and the catalyst was cooled down to room temperature, and heated again to 400 °C (solid lines in **Fig. 3A**). Afterwards the catalyst material was cooled down to room temperature, exposed to a specific probe molecule at 25 °C, and then heated to 400 °C in N_2 (dashed lines in **Fig. 3A**). **Fig. 3A** shows a comparison of the IR bands of SiH_x at various temperatures, before and after the exposure to probe molecules. To better illustrate the behavior of the SiH_x bands over time, we fitted the SiH_x bands as described in Section **S2** of the SI, and plotted the summed area of both bands over time (**Fig. 3B**). The reaction of SiH_x with methanol was fast and complete within one minute at 25 °C, while water removed all SiH_x at ~70 °C, and CO_2 did not affect the SiH_x bands appreciably in the temperature regime studied.

These results suggest that protic species can react with SiH_x: the reaction of methanol with SiH_x could lead to activation of the protic -OH bond, and production of H_2 and methoxy species. Similarly, water could form -OH groups and H_2. The observed trend in activity is consistent with the higher acidity of methanol in the gas phase compared to water, and possibly also explained by the more hydrophobic character of a (partially) hydridic silica surface.[19,55] However, this hypothesis could not be supported by conclusive evidence, as H_2 could not be detected via online mass spectrometry or gas chromatography during dosing of methanol or water. While we did observe what are most likely water and methoxy species via DRIFTS at ~ 1620 and ~ 1460 cm^{-1}, respectively, we refrain from interpreting these bands because the bands in the spectral region below 2000 cm^{-1} were heavily affected by the removal of hydrides, due to changes in the Si–O vibrational overtones and combination bands (**Fig. 3C**, grey spectrum).[37]

When subtracting the spectrum of Ni/SiO_2 at 40 °C after methanol addition with the spectrum before methanol addition with matching temperature, negative IR bands were seen at ~ 2010 and ~ 1880 cm^{-1} (**Fig. 3C**, shaded grey areas). When water was absorbed instead of methanol, the negative bands were still present but less intense (**Fig. 3C**, shaded pink areas). We believe this aspect deserves a word of caution, as using a spectrum of the pretreated catalyst as background is a common approach in operando spectroscopy.[4] Such negative IR bands fall in the same region where adsorbed CO, formate, formyl and (bi)carbonates bands are typically reported. This can lead to misinterpretation of operando spectra, especially at low temperatures. One must keep in mind that changes to the support due to temperature or wetting cause a change in IR signal.

As already pointed out by Meunier *et al*, when cooling down silica to 50 °C when using a background of the same sample at 350 °C, two bands appear at ~ 2036 and ~ 1902 cm^{-1}, which could be wrongly assigned to metal-carbonyl species.[56] However, we show here that even when using spectra of the same temperature as background,

chemical changes in the support can lead to differences in the support IR bands and thus to changes in the background or baseline of the resulting spectra. Due to the reaction of silicon oxyhydrides with probe molecules, the fundamental bands of Si-O-Si are most likely altered, leading to a change in the Si-O-Si overtones.

The presence of mobile and reactive hydrides on silica-supported metal catalysts has implications in hydrogenation-dehydrogenation catalysis. Silicon oxyhydrides are known to make the silica surface hydrophobic, a phenomenon used in, among others, chromatography.[19] This can influence the interactions of polar products and reactants with the silica surface, possibly affecting catalytic performance by favoring or suppressing adsorption near or at the active sites, and could change the interactions of metal nanoparticles with the silica surface itself, possibly affecting catalytic stability. Moreover, silicon oxyhydrides could act as a hydrogen reservoir and/or water scavenger during e.g., catalytic hydrogenation reactions.

Conclusion

It was found that silicon oxyhydride species are formed upon reduction of Ni/SiO_2 catalyst materials via a spillover of *H from Ni, as evidenced by the appearance of two infrared (IR) bands located at ~ 2275 and ~ 2257 cm^{-1} in the in-situ diffuse reflectance Fourier transform spectroscopy (DRIFTS) experiments, and further corroborated by density functional theory (DFT) calculations. The observed SiH_x bands disappeared with increasing temperature, consistently with a reversible, endothermic process having a reaction enthalpy in the range of 39–45 kJ/mol for SiH and of 24–28 kJ/mol for SiH_2. We propose that relatively stable silicon oxyhydrides convert into highly mobile hydrides species with increasing temperature, in line with studies of silicon hydrides in the semiconductors' literature. The order of magnitude of the observed enthalpy further suggests that hydrogen bonding is involved in such hydride mobilization process. We further investigated the reactivity of SiH_x species in Ni/SiO_2 catalysts by reaction with probe molecules. We showed that SiH_x species react quickly with methanol, more slowly with water and do not react with CO_2 at temperatures as high as 100 °C. The removal of the SiH_x species influenced the Si-O-Si IR bands, leading to severe distortion of IR spectra when using a spectrum of the reduced Ni/SiO_2 material as background. Hence, proper care has to be taken to avoid interpretation of these bands as carbonyl species, especially at low temperatures. All considered, the present study showcases the ability of SiO_2 to accommodate hydride species by spillover and suggests that the silica support can play an important and active role in heterogeneous catalysis.

Methods

Three Ni/SiO_2 catalyst materials were used, which have been labelled as 'small', 'medium' and 'large', depending on their Ni nanoparticle size: (i) 4.7 wt.% Ni/SiO_2 'small', with a 1.2 ± 0.5 nm mean Ni NP size; (ii) 11.8 wt.% Ni/SiO_2 'medium', with a 2.1 ± 1.1 nm mean Ni NP size; and (iii) 19.5 wt.% Ni/SiO_2 'large', with a 4.4 ± 2.4 nm mean Ni NP size. The synthesis and characterization of these three samples were described elsewhere.[4] CO_2 was provided by Linde at >99.99% purity. N_2 and H_2 were provided by Linde at >99.999% purity. Demineralized water was used and was sparged with N_2 for at least 30 min. Methanol was provided by Thermo Scientific at 99.8 % purity, dried over molecular sieves and sparged with N_2 for 30 min. The Ni/SiO_2 samples were loaded into a Harrick DRIFTS cell equipped with ZnSe windows and

pre-reduced at 550 °C (25 mL N_2/min, 25 ml H_2/min, 5 °C/min ramp rate), followed by cooling to room temperature in 40 mL/min N_2. The IR spectra were collected using a Bruker Tensor 27 FT-IR spectrometer. The gasses were supplied using a home-built gas rig connected to a bubbler for dosing water or methanol to the catalyst. For the probe molecule experiments, the pre-reduced catalyst was cooled down in N_2, after which the cell was heated again to 400 °C, and cooled to room temperature again. This first heating step was performed to check the reversibility of the SiH_x bands. After the second cool down step the probe molecule (i.e., water, methanol, or CO_2) was absorbed. Water and methanol were added by bubbling N_2 through the respective liquid. The bubbler with methanol was cooled to 0 °C to reach a similar vapor pressure compared to water (water: 32 mbar at 25 °C, methanol: 30 mbar at 0 °C)[57] in order to reach a similar concentration in stream. 5 mL/min N_2 was flowed through the bubbler for 2 min, and this gas stream was diluted with 35 mL/min N_2 to keep the total flow constant at 40 mL/min.

Author Contributions

The manuscript was written through contributions of all authors. All authors have given approval to the final version of the manuscript.

Funding Sources

This work is part of the Advanced Research Center for Chemical Building Blocks, ARC CBBC, which is co-founded and co-financed by the Netherlands Organization for Scientific Research (NWO) and the Netherlands Ministry of Economic Affairs and Climate Policy. B.B. acknowledges funding by the Austrian Science Fund (FWF) under the project number J4607–N.

Acknowledgements Martijn Hut (Utrecht University, UU) is thanked for performing some additional DFT calculations. Richard van de Sanden (Eindhoven University of Technology, TU/e) is thanked for valuable discussions on H mobility in Si and SiO_2. We thank Sebastian Weber (BASF SE), Nils Bottke (BASF SE) and Esther Groeneveld (BASF Nederland B.V.) for support of the research project.

References

(1) van Deelen, T. W.; Hernández Mejía, C.; de Jong, K. P. Control of Metal-Support Interactions in Heterogeneous Catalysts to Enhance Activity and Selectivity. *Nat. Catal.* **2019**, *2*, 955–970. https://doi.org/10.1038/s41929-019-0364-x.

(2) Yu, X.; Williams, C. T. Recent Advances in the Applications of Mesoporous Silica in Heterogeneous Catalysis. *Catal. Sci. Technol.* **2022**, *12*, 5765–5794. https://doi.org/10.1039/d2cy00001f.

(3) Ye, R. P.; Li, Q.; Gong, W.; Wang, T.; Razink, J. J.; Lin, L.; Qin, Y. Y.; Zhou, Z.; Adidharma, H.; Tang, J.; Russell, A. G.; Fan, M.; Yao, Y. G. High-Performance of Nanostructured Ni/CeO_2 Catalyst on CO_2 Methanation. *Appl. Catal. B Environ.* **2020**, *268*, 118474. https://doi.org/10.1016/j.apcatb.2019.118474.

(4) Vogt, C.; Groeneveld, E.; Kamsma, G.; Nachtegaal, M.; Lu, L.; Kiely, C. J.; Berben, P. H.; Meirer, F.; Weckhuysen, B. M. Unravelling Structure Sensitivity in CO_2 Hydrogenation over Nickel. *Nat. Catal.* **2018**, *1*, 127–134. https://doi.org/10.1038/s41929-017-0016-y.

(5) Khoobiar, S. Particle to Particle Migration of Hydrogen Atoms on Platinum-Alumina Catalysts from Particle to Neighboring Particles. *J. Phys. Chem.* **1964**, *68* (2), 411–412. https://doi.org/10.1021/j100784a503.

(6) Prins, R. Hydrogen Spillover. Facts and Fiction. *Chem. Rev.* **2012**, *112* (5), 2714–2738. https://doi.org/10.1021/cr200346z.

(7) Jenkinson, K.; Spadaro, M. C.; Golovanova, V.; Andreu, T.; Morante, J. R.; Arbiol, J.; Bals, S. Direct Operando Visualization of Metal Support Interactions Induced by Hydrogen Spillover During CO_2 Hydrogenation. *Adv. Mater.* **2023**, *35*, 2306447. https://doi.org/10.1002/adma.202306447.

(8) Cavanagh, R. R.; Yates, J. T.., Jr. Hydrogen Spillover on Alumina-A Study by Infrared Spectroscopy. *J. Catal.* **1981**, *68*, 22–26. https://doi.org/10.1016/0021-9517(81)90035-X.

(9) Karim, W.; Spreafico, C.; Kleibert, A.; Gobrecht, J.; Vandevondele, J.; Ekinci, Y.; Van Bokhoven, J. A. Catalyst Support Effects on Hydrogen Spillover. *Nature* **2017**, *541*, 68–71. https://doi.org/10.1038/nature20782.

(10) Beaumont, S. K.; Alayoglu, S.; Specht, C.; Kruse, N.; Somorjai, G. A. A Nanoscale Demonstration of Hydrogen Atom Spillover and Surface Diffusion across Silica Using the Kinetics of CO_2 Methanation Catalyzed on Spatially Separate Pt and Co Nanoparticles. *Nano Lett.* **2014**, *14* (8), 4792–4796. https://doi.org/10.1021/nl501969k.

(11) Prins, R.; Palfi, V. K.; Reiher, M. Hydrogen Spillover to Nonreducible Supports. *J. Phys. Chem. C* **2012**, *116* (27), 14274–14283. https://doi.org/10.1021/jp212274y.

(12) Dietz, R. E.; Selwood, P. W. Effect of Chemisorbed Hydrogen on the Magnetization of Nickel. *J. Chem. Phys.* **1961**, *35*, 270–281. https://doi.org/10.1063/1.1731899.

(13) Selwood, P. W. The Chemisorptive Bonding of Hydrogen on Nickel. *J. Catal.* **1976**, *42*, 148–161. https://doi.org/10.1016/0021-9517(76)90102-0.

(14) Martin, G. A.; Primet, M.; Dalmon, J. A. Reactions of CO and CO_2 on Ni/SiO_2 above 373 K as Studied by Infrared Spectroscopic and Magnetic Methods. *J. Catal.* **1978**, *53*, 321–330. https://doi.org/10.1016/0021-9517(78)90104-5.

(15) Wu, Z.; Cheng, Y.; Tao, F.; Daemen, L.; Foo, G. S.; Nguyen, L.; Zhang, X.; Beste, A.; Ramirez-Cuesta, A. J. Direct Neutron Spectroscopy Observation of Cerium

Hydride Species on a Cerium Oxide Catalyst. *J. Am. Chem. Soc.* **2017**, *139*, 9721–9727. https://doi.org/10.1021/jacs.7b05492.

(16) Wang, B.; Zhang, L.; Cai, J.; Peng, Z.; Cheng, P.; Li, X.; Zhang, H.; Yang, F.; Liu, Z. Formation and Activity Enhancement of Surface Hydrides by the Metal–Oxide Interface. *Adv. Mater. Interfaces* **2021**, *8*, 2002169. https://doi.org/10.1002/admi.202002169.

(17) Stephan, D. W. The Broadening Reach of Frustrated Lewis Pair Chemistry. *Science* **2016**, *354*, aaf7229. https://doi.org/10.1126/science.aaf7229.

(18) Wan Kim, T.; Kim, D.; Hyun Kim, S.; Suh, Y. W. Heterolytic H_2 Activation in Heterogeneous Hydrogenation/Hydroprocessing Catalysis. *ChemCatChem* **2024**, *16*, e202301581. https://doi.org/10.1002/cctc.202301581.

(19) Wagner, G. H.; Pines, A. N. Silicon Oxyhydride. *Ind. Eng. Chem.* **1952**, *44*, 321–326. https://doi.org/10.1021/ie50506a030.

(20) Copéret, C.; Estes, D. P.; Larmier, K.; Searles, K. Isolated Surface Hydrides: Formation, Structure, and Reactivity. *Chem. Rev.* **2016**, *116*, 8463–8505. https://doi.org/10.1021/acs.chemrev.6b00082.

(21) Buff, H.; Wohler, F. Ueber Neue Verbindungen Des Siliciums. *Justus Liebigs Ann. Chem.* **1857**, *104*, 94–109. https://doi.org/10.1002/jlac.18571040108.

(22) Bercherer, G.; During, O. Zur Struktur Des Dioxodisiloxans. *Naturwissenchaften* **1956**, *43*, 300. https://doi.org/10.1007/BF00629548.

(23) Tertykh, V. A.; Belyakova, L. A. Solid-Phase Hydrosilylation Reactions with Participation of Modified Silica Surface. *Stud. Surf. Sci. Catal.* **1996**, *99*, 147–189. https://doi.org/10.1016/s0167-2991(06)81020-7.

(24) Polo-Garzon, F.; Luo, S.; Cheng, Y.; Page, K. L.; Ramirez-Cuesta, A. J.; Britt, P. F.; Wu, Z. Neutron Scattering Investigations of Hydride Species in Heterogeneous Catalysis. *ChemSusChem* **2019**, *12*, 93–103. https://doi.org/10.1002/cssc.201801890.

(25) Morterra, C.; Low, M. J. D. Reactive Silica. I. The Formation of a Reactive Silica by the Thermal Collapse of the Methoxy Groups of Methylated Aerosil. *J. Phys. Chem.* **1969**, *73* (2), 321–326. https://doi.org/10.1021/j100722a008.

(26) Morterra, C.; Low, M. J. D. Reactive Silica. II. Nature of the Surface Silicon Hydrides Produced by the Chemisorption of Hydrogen. *J Phys Chem* **1969**, *73* (2), 327–333. https://doi.org/10.1021/j100722a009.

(27) Fisher, C.; Kriegsman, H. Chemisches Verhalten von Cyclischen Siloxanen Mit H_2SiO-Gruppen. *Z. Anorg. Allg. Chem.* **1969**, *367* (5–6), 233–242. https://doi.org/10.1002/zaac.19693670504.

(28) Seyferth, D.; Prud'Homme, C.; Wiseman, G. H. Cyclic Polysiloxanes from the Hydrolysis of Dichlorosilane. *Inorg. Chem.* **1983**, *22*, 2163–2167. https://doi.org/10.1021/ic00157a014.

(29) Engelhardt, G.; Jancke, H.; Lippmaa, E.; Samoson, A. Structure Investigations of Solid Organosilicon Polymers by High Resolution Solid State ^{29}Si NMR. *J. Organomet. Chem.* **1981**, *210*, 295–301. https://doi.org/10.1016/S0022-328X(00)80888-8.

(30) Quignard, F.; Lécuyer, C.; Choplin, A.; Olivier, D.; Basset, J. M. Surface Organometallic Chemistry of Zirconium: Application to the Stoichiometric Activation of the CH Bonds of Alkanes and to the Low-Temperature Catalytic Hydrogenolysis of Alkanes. *J. Mol. Catal.* **1992**, *74*, 353–363. https://doi.org/10.1016/0304-5102(92)80253-D.

(31) Vidal, V.; Théolier, A.; Thivolle-Cazat, J.; Basset, J. M.; Corker, J. Synthesis, Characterization, and Reactivity, in the C-H Bond Activation of Cycloalkanes, of a

Silica-Supported Tantalum(III) Monohydride Complex: (≡SiO)$_2$Ta^{III}-H. *J. Am. Chem. Soc.* **1996**, *118*, 4595–4602. https://doi.org/10.1021/ja953524l.

(32) Rataboul, F.; Baudouin, A.; Thieuleux, C.; Veyre, L.; Copéret, C.; Thivolle-Cazat, J.; Basset, J. M.; Lesage, A.; Emsley, L. Molecular Understanding of the Formation of Surface Zirconium Hydrides upon Thermal Treatment under Hydrogen of [(≡SiO)Zr(CH$_2$*t*Bu)$_3$] by Using Advanced Solid-State NMR Techniques. *J. Am. Chem. Soc.* **2004**, *126*, 12541–12550. https://doi.org/10.1021/ja038486h.

(33) Wackerow, W.; Thiam, Z.; Abou-Hamad, E.; Al Maksoud, W.; Hedhili, M. N.; Basset, J. M. Characterization of Silica-Supported Tungsten Bis- And Tris-Hydrides by Advanced Solid-State NMR. *J. Phys. Chem. C* **2021**, *125*, 12819–12826. https://doi.org/10.1021/acs.jpcc.1c03625.

(34) Maity, N.; Barman, S.; Callens, E.; Samantaray, M. K.; Abou-Hamad, E.; Minenkov, Y.; D'Elia, V.; Hoffman, A. S.; Widdifield, C. M.; Cavallo, L.; Gates, B. C.; Basset, J. M. Controlling the Hydrogenolysis of Silica-Supported Tungsten Pentamethyl Leads to a Class of Highly Electron Deficient Partially Alkylated Metal Hydrides. *Chem. Sci.* **2016**, *7*, 1558–1568. https://doi.org/10.1039/c5sc03490f.

(35) Van Meerbeek, A.; Jelli, A.; Fripiat, J. J. Reduction of the Surface of Silica Gel by Hydrogen Spillover. *J. Catal.* **1977**, *46*, 320–325. https://doi.org/10.1016/0021-9517(77)90215-9.

(36) Vogt, C.; Meirer, F.; Monai, M.; Groeneveld, E.; Ferri, D.; van Santen, R. A.; Nachtegaal, M.; Unocic, R. R.; Frenkel, A. I.; Weckhuysen, B. M. Dynamic Restructuring of Supported Metal Nanoparticles and Its Implications for Structure Insensitive Catalysis. *Nat. Commun.* **2021**, *12*, 7096. https://doi.org/10.1038/s41467-021-27474-3.

(37) Yan, W.; Lv, M.; He, M.; Liu, X. Effect of Second Si–O Vibrational Overtones/Combinations on Quantifying Water in Silicate and Silica Minerals Using Infrared Spectroscopy, and an Experimental Method for Its Removal. *Phys. Chem. Miner.* **2022**, *49*, 5. https://doi.org/10.1007/s00269-022-01179-5.

(38) Becke, A. D. Density-functional Thermochemistry. III. The Role of Exact Exchange. *J. Chem. Phys.* **1993**, *98* (7), 5648–5652. https://doi.org/10.1063/1.464913.

(39) Ditchfield, R.; Hehre, W. J.; Pople, J. A. Self-Consistent Molecular-Orbital Methods. IX. An Extended Gaussian-Type Basis for Molecular-Orbital Studies of Organic Molecules. *J. Chem. Phys.* **1971**, *54* (2), 724–728. https://doi.org/10.1063/1.1674902.

(40) Whittaker, T.; Kumar, K. B. S.; Peterson, C.; Pollock, M. N.; Grabow, L. C.; Chandler, B. D. H_2 Oxidation over Supported Au Nanoparticle Catalysts: Evidence for Heterolytic H_2 Activation at the Metal–Support Interface. *J. Am. Chem. Soc.* **2018**, *140*, 16469–16487. https://doi.org/10.1021/jacs.8b04991.

(41) Aireddy, D. R.; Ding, K. Heterolytic Dissociation of H_2 in Heterogeneous Catalysis. *ACS Catal.* **2022**, *12*, 4707–4723. https://doi.org/10.1021/acscatal.2c00584.

(42) Zhuravlev, L. T. The Surface Chemistry of Amorphous Silica. Zhuravlev Model. *Colloids Surf. Physicochem. Eng. Asp.* **2000**, *173*, 1–38. https://doi.org/10.1016/S0927-7757(00)00556-2.

(43) Davydov, A. *Molecular Spectroscopy of Oxide Catalyst Surfaces*; John Wiley & Sons Ltd, West Sussex, **2003**. https://doi.org/10.1002/0470867981

(44) Kurtz, H. A.; Karna, S. P. Hydrogen Cracking in SiO_2: Kinetics for H_2 Dissociation at Silicon Dangling Bonds. *J. Phys. Chem. A* **2000**, *104* (20), 4780–4784. https://doi.org/10.1021/jp993804d.

(45) Morrow, B. A.; McFarlan, A. J. Surface Vibrational Modes of Silanol Groups on Silica. *J. Phys. Chem.* **1992**, *96*, 1395–1400. https://doi.org/10.1021/j100182a068.
(46) Tully, J. C.; Chabal, Y. J.; Raghavachari, K.; Bowman, J. M.; Lucchese, R. R. Infrared Linewidths and Vibrational Lifetimes at Surfaces: H on Si(100). *Phys. Rev. B* **1985**, *31*, 1184–1186. https://doi.org/10.1103/PhysRevB.31.1184.
(47) Staebler, D. L.; Wronski, C. R. Reversible Conductivity Changes in Discharge-Produced Amorphous Si. *Appl. Phys. Lett.* **1977**, *31*, 292–294. https://doi.org/10.1063/1.89674.
(48) Peeters, F. J. J.; Zheng, J.; Aarts, I. M. P.; Pipino, A. C. R.; Kessels, W. M. M.; van de Sanden, M. C. M. Atomic Hydrogen Induced Defect Kinetics in Amorphous Silicon. *J. Vac. Sci. Technol. A* **2017**, *35*, 05C307. https://doi.org/10.1116/1.4987152.
(49) Branz, H. M. Hydrogen Collision Model of Light-Induced Metastability in Hydrogenated Amorphous Silicon. *Solid State Commun.* **1998**, *105*, 387–391. https://doi.org/10.1016/S0038-1098(97)10142-9.
(50) Branz, H. M.; Asher, S. E.; Nelson, B. P. Light-Enhanced Deep Deuterium Emission and the Diffusion Mechanism in Amorphous Silicon. *Phys Rev B* **1993**, *47*, 7061–7066. https://doi.org/10.1103/PhysRevB.47.7061.
(51) Nickel, N. H. Hydrogen Diffusion through Silicon/Silicon Dioxide Interfaces. *J. Vac. Sci. Technol. B* **2000**, *18*, 1770–1772. https://doi.org/10.1116/1.591469.
(52) Garrone, E.; Ugliengo, P. Silanol as a Model for the Free Hydroxyl of Amorphous Silica: Non-Empirical Calculations of the Vibrational Features of H_3SiOH. *Stud. Surf. Sci. Catal.* **1989**, *48*, 405–413. https://doi.org/10.1016/S0167-2991(08)60703-X.
(53) Qian, C.; Sun, W.; Hung, D. L. H.; Qiu, C.; Makaremi, M.; Hari Kumar, S. G.; Wan, L.; Ghoussoub, M.; Wood, T. E.; Xia, M.; Tountas, A. A.; Li, Y. F.; Wang, L.; Dong, Y.; Gourevich, I.; Singh, C. V.; Ozin, G. A. Catalytic CO_2 Reduction by Palladium-Decorated Silicon–Hydride Nanosheets. *Nat. Catal.* **2019**, *2*, 46–54. https://doi.org/10.1038/s41929-018-0199-x.
(54) Sun, W.; Qian, C.; He, L.; Ghuman, K. K.; Wong, A. P. Y.; Jia, J.; Jelle, A. A.; O'Brien, P. G.; Reyes, L. M.; Wood, T. E.; Helmy, A. S.; Mims, C. A.; Singh, C. V.; Ozin, G. A. Heterogeneous Reduction of Carbon Dioxide by Hydride-Terminated Silicon Nanocrystals. *Nat. Commun.* **2016**, *7*, 12553. https://doi.org/10.1038/ncomms12553.
(55) Gao, D. Acidities of Water and Methanol in Aqueous Solution and DMSO. *J. Chem. Educ.* **2009**, *86* (7), 864. https://doi.org/10.1021/ed086p864.
(56) Paredes-Nunez, A.; Jbir, I.; Bianchi, D.; Meunier, F. C. Spectrum Baseline Artefacts and Correction of Gas-Phase Species Signal during Diffuse Reflectance FT-IR Analyses of Catalysts at Variable Temperatures. *Appl. Catal. Gen.* **2015**, *495*, 17–22. https://doi.org/10.1016/j.apcata.2015.01.042.
(57) Haynes, W. M. *Handbook of Chemistry and Physics*; 95th ed.; CRC Press, Boca Raton, FL, **2014**. https://doi.org/10.1201/b17118